Design and fabrication of an InP arrayed waveguide grating for monolithic PICs*

Pan Pan(潘盼), An Junming(安俊明)†, Wang Liangliang(王亮亮), Wu Yuanda(吴远大), Wang Yue(王玥), and Hu Xiongwei(胡雄伟)

State Key Laboratory on Integrated Optoelectronics, Institute of Semiconductors, Chinese Academy of Sciences, Beijing 100083, China

Abstract: A 10-channel, 200 GHz channel spacing InP arrayed waveguide grating was designed, and the deep ridge waveguide design makes it polarization independent. Under the technologies of molecular beam epitaxy, lithography, and induced coupler plasma etching, the chip was fabricated in our laboratory. The test results show that the insertion loss is about –8 dB, and the crosstalk is less than –17 dB.

Key words: InP AWG; monolithic PICs; polarization independence
DOI: 10.1088/1674-4926/33/7/074010 **EEACC:** 2570

1. Introduction

Photonic integrated circuits (PICs) have been developed for reducing cost and power consumption in the optical communications field[1, 2]. A PIC integrates multiple active and passive components such as lasers, modulators, detectors, multiplexers/demultiplexers and optical amplifiers. The PIC eliminates the need for a large number of optical components and complex electronic signal processing, achieves greater network reliability and the fiber capacity benefits from complex modulation while consuming significantly less space and power than traditional systems. It is important to fabricate reproducible, high-quality active and passive waveguide transitions in PIC technology[3, 4]. InP is a very powerful platform, giving efficient optical gain, high-speed switching and modulation with low voltages, and efficient high-speed detection. Monolithic integration in InP has been proven to save significant cost, power, and footprint. Multi-wavelengths and multi-signals transmitting/receiving must be able to be handled by complex InP PICs. As a multiplexer/demultiplexer, the InP arrayed waveguide grating (AWG) is an important passive device. The world's first InP 8 × 8 monolithic tunable optical router (MOTOR) operating at 40 Gbps line rate per port was designed with AWG, SOAs and so on[6]. It has been reported that a 40-channel InP AWG was integrated with 40 electroabsorption modulated lasers (EMLs), including 241 discrete function components on a single monolithic InP chip. In addition, a multi-channel coherent PM-QPSK InP transmitter operating at 112 Gb/s per wavelength was also reported[7, 8].

Over the years, many researchers in China have made some great achievements in the research of discrete photonic devices. However, our integrated photonic devices are still at the earliest stages of development. We have mastered the key technology of PICs, but a complex PIC chip has never been reported. Power consumption and access to cost-effective energy in conjunction with the continued expansion of the internet are becoming the most critical issues in the communication industry today. To satisfy the demand of ever-increasing communication capacity in broadband communication systems and lower costs, PIC technology is of great importance. Here, we present a 10-channel InP-based AWG which will be integrated with distributed feedback (DFB) lasers and electroabsorption modulators (EAMs) in InP monolithic PICs. It is the first trial in China. It is of great importance in the development of PIC technology and has a far-reaching impact on the optical network in China.

2. Design and fabrication

To avoid polarization dependence and reduce bending radii, a deep ridge InGaAsP/InP waveguide structure has been adopted[9]. The width of the waveguide is determined by the polarization of the waveguide and the bandgap of InGaAsP. Waveguides with lower bandgaps and larger width can easily achieve polarization independence, and have a good fabrication tolerance. On the other hand, to satisfy the single mode condition, the waveguide width should be decreased. We choose a suitable width to balance the two aspects. In addition, a kind of tapered waveguide is adopted in the slab region to decrease the coupling loss. The deep ridge waveguide consists of a 2-μm InP buffer layer, a 0.5-μm InGaAsP core layer with 1.05Q, and a 1.5-μm InP overcladding layer. The refractive index of InP is 3.1649 and the InGaAsP core layer with 1.05Q needs to be calculated as follows. The relationship of the lattice constant and different components of the quaternary compound is determined by Figaro's law. Suppose a is the lattice constant, InP ($E_g(0) = 1.421$ eV, $a = 0.5886$ nm), GaAs ($E_g(0) = 1.519$ eV, $a = 0.5653$ nm), InAs ($E_g(0) = 0.420$ eV), GaP ($E_g(0) = 2.338$ eV). For $In_xGa_{1-x}As_yP_{1-y}$ (x and y refer to the percentages of In and As in the quaternary compound),

$$a(x, y) = 5.8696 - 0.4184x + 0.1894y + 0.013xy. \quad (1)$$

To meet lattice matching, $a(x, y) = a(\text{InP})$, we get

* Project supported by the National High Technology Research and Development Program of China (No. 2011AA010303) and the National Natural Science Foundation of China (Nos. 61090390, 60837001, 60877014, 60776057).
† Corresponding author. Email: junming@red.semi.ac.cn
Received 17 January 2012, revised manuscript received 14 February 2012 © 2012 Chinese Institute of Electronics

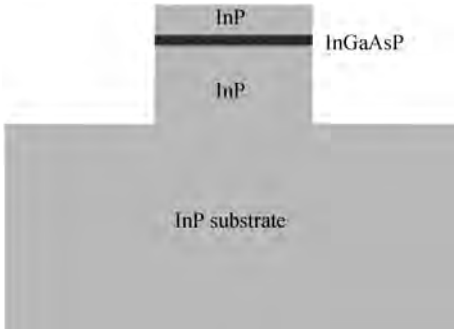

Fig. 1. Cross-sectional diagram of the deep-ridge waveguide with polarization independence.

Table 1. Design parameters of InP AWG.

Parameter name	Value
Number of channels	8 in, 12 out
Number of arms	55
Waveguide width	2.45 μm
Etching depth	5 μm
Channel spacing ($\Delta\lambda$)	1.6 nm
Radius of Rowland circle (R)	1133.8 μm
Path-length difference (ΔL)	35.544 μm
Bend radius	250 μm
Gap between tapered wav. at slab regions	1.5 μm

$$x = \frac{0.4526y}{1 - 0.031y}. \tag{2}$$

$1.05Q$ means that the emission wavelength is 1.05 μm, so band gap $E_g = 1.24/1.05 = 1.18095$ eV.

The formula for calculating the refractive index of a quaternary compound is as follows:

$$n^2 = 1 + \frac{E_d}{E_0} + \frac{E_d}{E_0^3}E^2 + \frac{\eta}{\pi}E^4 \ln\frac{2E_0^2 - E_g^2 - E^2}{E_g^2 - E^2}, \tag{3}$$

$$\eta = \frac{\pi E_d}{2E_0^3(E_0^2 - E_g^2)}. \tag{4}$$

Here,

$$\begin{aligned} E_0 &= 3.391 - 1.652y + 0.83y^2 - 0.123y^3, \\ E_d &= 28.91 - 9.278y + 5.626y^2, \\ E_g &= 1.35 - 0.72y + 0.12y^2. \end{aligned} \tag{5}$$

The formula above has adopted the lattice matching condition:

$$y = 2.197x. \tag{6}$$

According to the calculations above, we get $y = 0.24477$, then we know that the chemical formula of the quaternary compound is $In_{0.11141}Ga_{0.88859}As_{0.24477}P_{0.75523}$, and the refractive index of the core layer is 3.2530[10]. To reduce absorption loss, an undoped or SI-InP overcladding layer is also required. The deep-ridge structure shown in Fig. 1 makes the bending radii be only 250 μm, enabling us to fabricate an extremely small InP AWG. For integration with 10 DFBs and EAMs, the output side (in the bottom of the chip) is provided with 10 waveguides, which are separated by a distance of 250 μm at the edge of the chip, while the input side to the AWG is provided with 9 waveguides. The channel spacing between the adjacent channels is designed to be 1.6 nm (200 GHz). To reduce the chances of failure during processing and packaging, we add the number of output ports to 13. The concrete design parameters are shown in Table 1, and the layout of the InP AWG that we designed is shown in Fig. 2. In order to be convenient for testing, we put one of the 9 channels on the opposite side of the output ports, and so do the output ports. The grating array consists of 55 waveguides. The compact design makes the typical size of the device 4×4 mm^2.

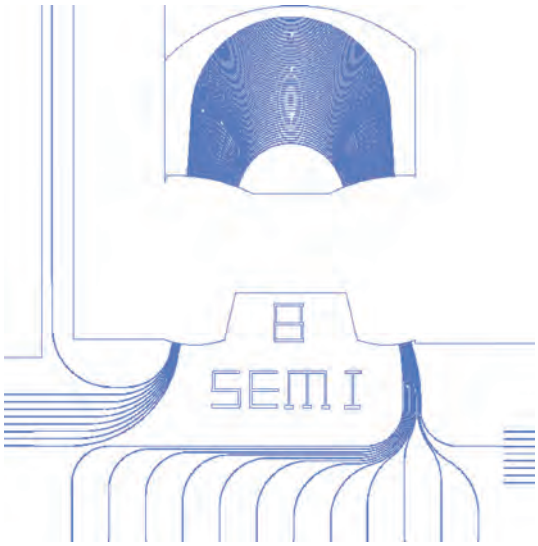

Fig. 2. Layout of the 10-channel InP AWG.

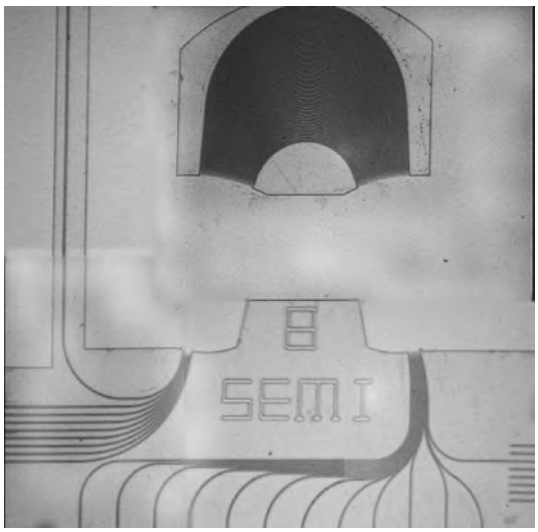

Fig. 3. Photograph of the fabricated AWG.

The InP buffer layer, InGaAsP core layer, and InP overcladding layer are grown epitaxially in sequence on a InP semi insulating substrate. The InP AWG is then formed using lithography and induced coupler plasma technologies. Figure 3 shows the photograph of InP-based AWG fabricated in our laboratory, and Figure 4 shows the SEM image of the side walls of the waveguides. We can see that the sidewalls of the buffer

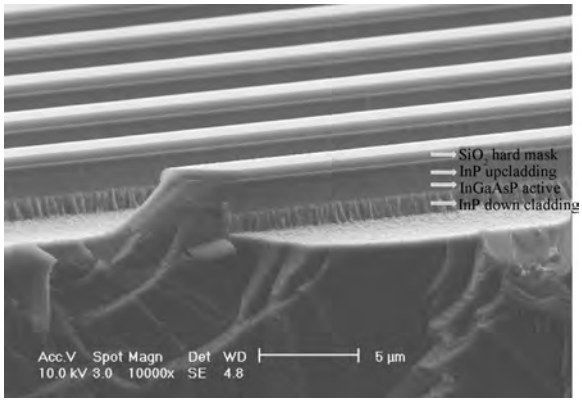

Fig. 4. Cross-sectional SEM image of the fabricated AWG.

layer, core layer and overcladding layer are not very smooth, the propagation losses are somewhat high because our guiding structure is very sensitive to side-wall roughness.

3. Results and discussion

We measured the devices by launching ASE light from a 1.55 μm range fiber into the input port of the AWG which is in the opposite side of the output ports, and then detecting it in the output ports with a spectrum analyzer, by moving the output fiber from one channel to the next after each wavelength scan. Figure 5(a) shows the spectral response of the 10 channels of an InP-based AWG with 200 GHz channel spacing. After deducting the loss of the straight waveguide, the measured insertion loss is about –8 dB at the central output port and the crosstalk is less than –17 dB. Figure 5(b) shows the free spectrum diagram of the central port and the free spectra range (FSR) is 10.52 μm, which is marked in the figure. The central wavelength is not spaced accurately at 1.55 μm. Firstly, this is because the input port is not the central one, for the routing principle of AWG, the central wavelength would shift; Secondly, fabrication errors of the effective index and differences in length of the arrayed waveguides can also cause wavelength shift [11]. The nonuniformity between central and side channels is less than 3 dB. As an AWG can be used as a multiplexer or a demultiplexer, we measured it as the output ports are input ports and input ports are output ports. Figures 5(c) and 5(d) show the spectral responses of the 8 input channels and the central channel, respectively. The FSR is 19.36 nm, which is very close to the designed value. And the small difference of FSR between the two measurements is due to fabrication errors. The insertion loss is almost the same to the former. Nevertheless, both the two measurements show that the channels are not very accurately spaced in wavelength, but with a separation error of $\pm$0.3 nm while the designed value is 1.6 nm. It is mainly because the fabrication errors in the effective index of the slab waveguides, the gap between arrayed waveguides and the radius of Rowland circle. The average value of 3-dB bandwidth of the left-side channels is 0.95 nm, while the underneath side channels is 1.75 nm. The big difference is due to the instability of different chips and different test environments.

We have also tested the polarization dependence of the fabricated chip. The measurement was carried out for the TM and

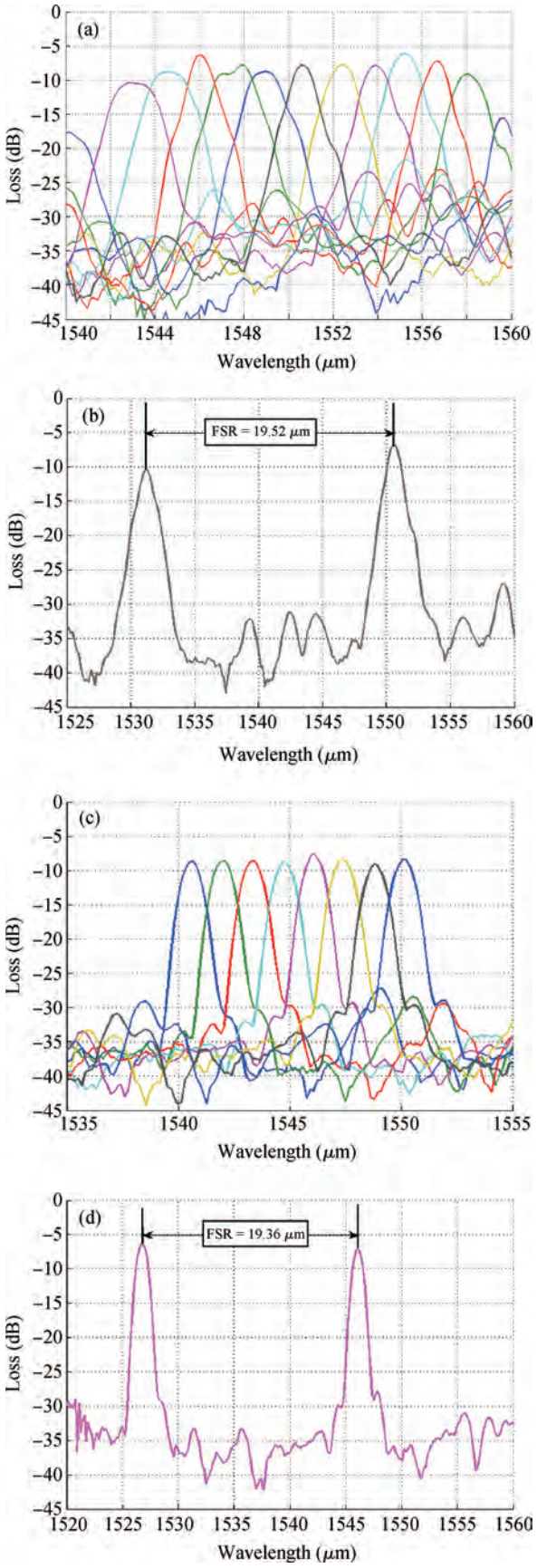

Fig. 5. (a, b) All-channel and central channel transmission spectra with the underneath side is output port and (c, d) the left side is output port. The FSR is marked at the central channel transmission spectrum.

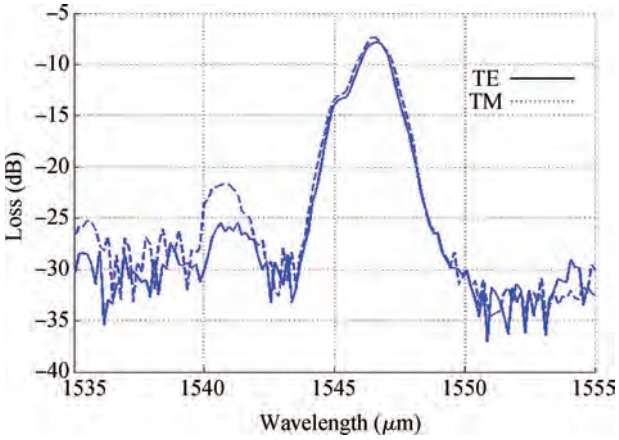

Fig. 6. TE and TM spectra of the central channel.

TE modes, respectively. Figure 6 shows the TE and TM spectrum response. The analysis results show that the devices have good polarization independence and residual polarization dispersion of all channels is smaller than 0.2 nm, which is negligible compared to the channel spacing of 200 GHz (1.6 nm).

In this experiment, all the waveguides are exposed in the air, so the tested results can be influenced easily by the external environment. In the next step, we will add a SiO_2 protecting layer on the InP overcladding layer to protect the waveguides from external influence.

4. Conclusion

We designed, fabricated and characterized a 10-channel AWG with 1.6 nm (200 GHz) channel spacing at 1.55 μm wavelength. A deep ridge waveguide structure is adopted to achieve polarization independence. The compact design makes the chip size be only 4×4 mm^2. The insertion loss is about –8 dB at the central output port and the crosstalk is less than –17 dB. Adding a protecting layer on the waveguides can further reduce the propagation loss. Therefore, the chip will be widely used in monolithic PICs.

References

[1] Suzaki Y. Quantum electron. IEEE J, 2005, 11(1): 43
[2] Zhou W M, Shen H, Ervin M H, et al. Monolithically integrated semiconductor active and passive optical waveguide devices grown by selective epitaxy. Optoelectronic Integrated Circuits IV, 2005, 3950: 118
[3] Ho S T, Huang Y Y, Ma J. InP photonic integrated circuit and DWDM-on-chip technology. IEEE Avionics, Fiber-Optics and Photonics Technology Conference, 2007: 56
[4] Nagarajan R, Joyner C H, Schneider R P, et al. Large-scale photonic integrated circuits. IEEE J Sel Topics Quantum Electron, 2005, 11: 50
[5] Lu P, De M L, Chen J, et al. Novel polarization-insensitive wavelength multiplexer demultiplexer modules. Microw Opt Technol Lett, 2003, 38: 42
[6] Nicholes S C, Mašanovi M L, Jevremovi B, et al. The world's first InP 8×8 monolithic tunable optical router (MOTOR) operating at 40 Gbps line rate per ports. OFC: Conference on Optical Fiber Communication, 2009, 1(5): 3078
[7] Welch D F, Kish F A, Nagarajan R, et al. The realization of large-scale photonic integrated circuits and the associated impact on fiber-optic communication systems. J Lightwave Technol, 2006, 24: 4674
[8] Evans P, Fisher M, Malendevich R, et al. Multi-channel coherent PM-QPSK InP transmitter photonic integrated circuits (PICs) operating at 112 Gb/s per wavelength. Conference on Optical Fiber Communication, 2011: 3
[9] Bissessur H, PagnodRossiaux P, Mestric R, et al. Extremely small polarization independent phased-array demultiplexers on InP. IEEE Photonics Technol Lett, 1996, 8: 554
[10] Lei Hongbing. The research of arrayed waveguide grating as multiplexer/demultiplexer. Postdoctoral Degree Thesis, Institute of Semiconductors of the Chinese Academy of Sciences, 2000 (in Chinese)
[11] An Junming, Xia Junzhi, Li Jian, et al. Numerical analysis for phase error of silica-based arrayed waveguide grating. Chinese Journal of Semiconductors, 2005, 26: 220